Journal of Mining and Earth Sciences Vol.54 (2016) 10-16

Journal of Mining and Earth Sciences

Journal homepage: http://tapchi.humg.edu.vn/en/home.html

Density-driven instability of miscible fluids in porous media with horizontal flow

Trieu Hung Truong[1,*], J. R. Angilella[2], C. Oltéan[3] and M. Buès[3]

[1] *Hanoi University of Mining and Geology, Vietnam*
[2] *Université de Caen - ESIX/LUSAC, France*
[3] *Université de Lorraine, France*

ARTICLE INFO

Article history:
Received 16 November 2015
Accepted 10 April 2016
Available online 30 July 2016

Keywords:
Porous medium
Density-driven
Instability
Miscible

ABSTRACT

A linear stability analysis of uniform parallel flow superposed to a quasi-steady horizontal layer of solute is presented. It is shown that the plume is convectively unstable for the parameters considered here, and confirms the stabilizing effect of the longitudinal dispersivity or the destabilizing effect of the solute concentration, in agreement with previous experimental or numerical analyses.

1. Linear stability analysis

In order to enhance our understanding of solute sedimentation in an underground flow of pure water (Dane et al., 1994; Oltéan et al., 2004; Schincariol et al., 1990, 1994; Truong et al., 2010; Min, 2015), a simplified uniform horizontal flow is considered with velocity $V_\infty \vec{e}_x$, as shown in Figure 1 which transports a horizontal layer of solute with initial thickness λ. This elementary unsteady solution of the motion equations, denoted by $\vec{V}^0$, $\hat{P}^0(x,y)$ and $C_m^0(y,t)$, satisfies in the following equations

$$\frac{\partial \hat{P}^0}{\partial x} = const \tag{1}$$

$$\vec{V}^0 = -\frac{k_0}{\mu}\frac{\partial \hat{P}^0}{\partial x}\vec{e}_x = V_\infty \vec{e}_x \tag{2}$$

$$\frac{\partial C_m^0}{\partial t} = D_m \frac{\partial^2 C_m^0}{\partial y^2} \tag{3}$$

and takes the following classical form

$$C_m^0(y,t) = \frac{C_{inj}}{2}\left(erf\,\frac{y+\lambda/2}{2\sqrt{D_m t}} - erf\,\frac{y-\lambda/2}{2\sqrt{D_m t}} \right) \tag{4}$$

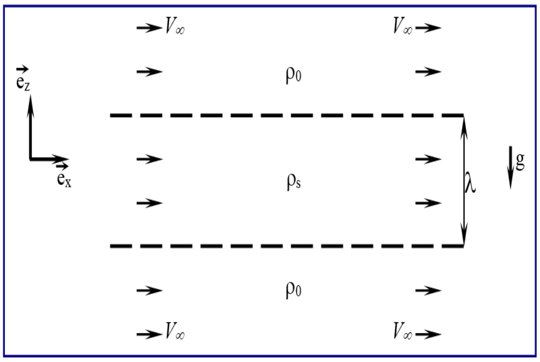

Figure 1. Sketch of the simplified flow in porous medium used for the linear stability analysis. The density of the injected solute is r_s, and r_0 is the density of pure water

This solution is independent on the longitudinal dispersivity of the medium, since density gradients are perpendicular to the uniform flow. Also, a vertical pressure gradient base flow depends on the following control parameters: the zonal velocity $V_\infty \vec{e}_x$, the injected

* *Corresponding author. Tel.:* +84 963990202
Email: trieuhungtruong@humg.edu.vn

flow rate Q_{inj} (linked to the thickness λ of the layer by $Q_{inj} = V_\infty \lambda b$), and the injected concentration C_{inj}. Our goal is to check the effect of these parameters on the stability of the plume by means of a linear stability analysis.

2. Linearized equations and normal modes

The base flow described above is unsteady, since the solute diffuses into fresh water. Nevertheless, assume that this process is sufficiently slow and then investigation is proposed for the evolution of the plume over time scales that are much shorter than the diffusive time scale $t = \lambda^2 / D_m$. Since t is of the order of few convective time scales, this assumption requires that the Péclet number is large enough. Under this quasi-static approximation, the concentration field in Equation (4) is approximated by a steady solution. By replacing the diffusive scale $\sqrt{D_m t}$ by a constant thickness $d_0 = l$ and injecting the perturbed fields

$$\vec{V}(x,y,t) = \vec{V}^0 + \vec{V}^1(x,y,t), \tag{5}$$

$$\hat{P}(x,y,t) = \hat{P}_0(x,y) + \hat{P}^1(x,y,t), \tag{6}$$

$$C_m(x,y,t) = C_m^0(y) + C_m^1(x,y,t), \tag{7}$$

into the complete motion equations, and neglecting quadratic terms result in

$$Ñ.\vec{V}^1 = 0, \tag{8}$$

$$\vec{V}^1 = -\frac{k_0}{\mu}\left(Ñ\hat{P}^1 + r_0 \gamma C_m^1 g \vec{e}_y\right), \tag{9}$$

$$\frac{\partial C_m^1}{\partial t} + \vec{V}^1.\nabla C_m^0 + \vec{V}^0.\nabla C_m^1 = D_m \Delta C_m^1 + \\ + \frac{b^2}{210 D_m} u_0 \left(1 + \gamma C_m^0\right) \times (u_0 C_{m,xx}^1 + C_{m,y}^0 v_{1,x}) \tag{10}$$

where the comma indicates a partial derivative with respect to state variables and the associated boundary conditions correspond to the absence of perturbation at infinity as

$$C_m^1(x, y = \pm\infty) = u_1(x, y = \pm\infty) \\ = v_1(x, y = \pm\infty) = 0 , \tag{11}$$

Examining for solutions in the form of normal modes (Betchov and Criminale, 1967), one can re-write as

$$u_1(x,y,t) = q(y)e^{i(kx-\omega t)} + q^*(y)e^{-i(k^* x-\omega t)}, \tag{12}$$

$$v_1(x,y,t) = p(y)e^{i(kx-\omega t)} + p^*(y)e^{-i(k^* x-\omega t)}, \tag{13}$$

$$C_m^1(x,y,t) = f(y)e^{i(kx-\omega t)} + f^*(y)e^{-i(k^* x-\omega t)}, \tag{14}$$

$$\text{with } f(\pm\infty) = q(\pm\infty) = p(\pm\infty) = 0, \tag{15}$$

In these equations, the symbol "*" indicates a complex conjugate, $k = k_r + i k_i$ is the complex wavenumber, and ω (real) is the pulsation of the perturbation. Also, the wavenumber of the Darcy equation is considered to be valid if $b = 2\pi / k_r$ and $b = 2\pi / k_i$. By substituting this modal decomposition into the linearized Equations (8), (9), (10), a non-dimensional form is achieved by using b for lengths and b / V_∞ for times, as shown in equation (16).

$$p' + ikq = 0 \\ ikp - q' + V_g ikf = 0 \\ (ik - i\omega) f + pC_{m,y}^0 = \frac{1}{Pe}\left[-k^2 f + f''\right] + \\ + \frac{Pe}{210}\left[-k^2 f + ikpC_{m,y}^0\right] \tag{16}$$

where the pressure has been eliminated by taking the curl of the Darcy equation. The non-dimensional numbers appearing in these equations are the Péclet number (*Pe*) and the non-dimensional sedimentation velocity (*Vg*):

$$P_e = \frac{V_\infty b}{D_m}, \tag{16a}$$

$$V_g = \frac{k_0 \rho_0 \gamma C_{inj} g}{\mu V_\infty}, \tag{16b}$$

Note that the non-dimensional thickness of the unperturbed layer is denoted $\bar{l} = l / b$ for the remaining of the paper. As noted above, this parameter is used to determine the flow rate of solute injected in the cell.

Equations (16) are solved by using finite differences on a vertical grid of the form $-L < y_1 < .. < y_N < L$, where L is a large vertical scale**.** a quadratic eigenvalue problem is obtained for the vector consisting of the unknowns at the grid points

$$\vec{X} = \begin{bmatrix} (f(y_i))_{i=1,N}, (f'(y_i))_{i=1,N}, \\ ,(q(y_i))_{i=1,N}, (p(y_i))_{i=1,N} \end{bmatrix}$$

of the form as

$$M_1\,\vec{X} + k\,M_2\,\vec{X} = k^2\,N\,\vec{X}$$

where the matrices M_1, M_2 and N contain the coefficients appearing in (16). This quadratic problem can be reduced to a generalized eigenvalue problem of the form $A\vec{Z} = kB\vec{Z}$ by the work (Suslov, 2006). Therefore, the four parameters $V_g,\ P_e,\ \lambda,\ \omega$ appearing in Equation (16) are fixed and solving the eigenvalue problem obtains both the eigenvalues k and the corresponding eigenvectors $\vec{X}$. The 4N eigenvalues and eigenvectors are given by the numerical solver, the "physical ones" is chosen to satisfy two arbitrary criteria: (i) the growth rate $-k_i$ should not be too large, (ii) the wavelength $2\pi / k_r$ must be larger than 1, the non-dimensional gap of the cell, and is not also too large.

3. Effect of the longitudinal dispersivity

In order to check the effect of dispersivity on the stability of the plume, the growth rate of the perturbation are calculated with an isotropic tensor by removing the term *Pe/210* from Equation (16) and with a non-isotropic tensor by taking account of Taylor dispersion by keeping this term in Equation (16).

The non-dimensional parameters are selected as *Pe = 22*, $\bar{\lambda}$ =7.6 and *Vg = 0.58*, which correspond to the values V_∞ = 0.06mm/s, Q_{inj} = 0.5mL/h, and C_{inj} = 0.3 g/L. Results are shown in Figure 2.

From the analysis of results in Figure 2a, one can conclude that the dispersion relation is affected by the longitudinal dispersion. The longitudinal dispersivity has a stabilizing effect. Both the growth rate of the instability and the range of unstable pulsations are reduced when $\alpha_L \neq 0$. In addition, Figure 2b shows that the phase velocity $c = \omega/k_r$ is almost constant and equal to 1. This suggests that the waves are non-dispersive and move at the velocity of the zonal flow in the absence of Taylor dispersion. In contrast, when $\alpha_L \neq 0$, the phase velocity is no longer constant and the group velocity $d\omega/dk_r$ is different from *c* and waves are dispersive. The pulsation of the most unstable mode is $\omega \approx 1$ in the isotropic case and $\omega \approx 0.5$ in the non-isotropic case. The wavenumber of this mode can be read in Figure 2b with $k_r \approx 1$ in the isotropic case and $k_r \approx 0.5$ in the non-isotropic case. The wavelength of the most unstable mode is therefore larger when the Taylor dispersion is taken into account. For the parameters considered here, a wavelength is achieved about 6 mm in the isotropic case and 12mm in the non-isotropic case. The latter value is in agreement with our experimental results (Trieu et al., 2010), whereas the former value is much too short.

(a): a $_L$ ¹ 0*;*   *(b):* a $_L$ = 0

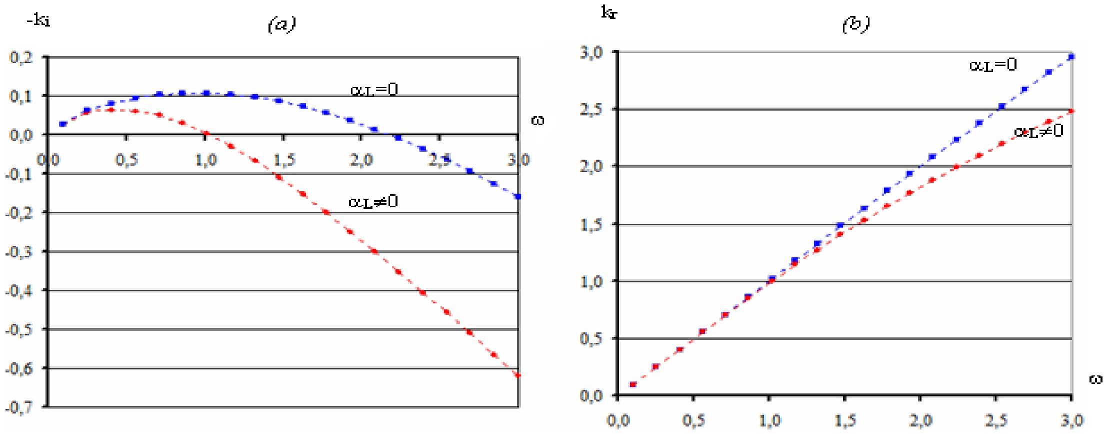

Figure 2. Growth rate - k_i and wavenumber k_r versus the pulsation ω ,
for an isotropic dispersion tensor ($\alpha_L = 0$) and for a non-isotropic tensor ($\alpha_L \neq 0$)
The non-dimensional parameters are Pe = 22, $\bar{\lambda}$ =7.6 and Vg = 0.58

4. Effect of the injected concentration

In this section, the parameters $Pe = 22$ (that is $V_\infty = 0.06mm/s$) and $\bar{\lambda} = 7,6$ (that is $Q_{inj} = 0.5mL/h$) are fixed and five values for Vg between 0.14 and 1.44 (that is C_{inj} between $0.05g/L$ and $0.5g/L$) are chosen for calculation. Results are shown in Figure 4. Observe that the concentration has a destabilizing effect as the growth rate $-k_i$ is increased.

Figure 5a shows that the growth rate $-k_i^{max}$ of the most unstable mode increases with V_g . This is in agreement with the experimental and numerical observations (Trieu et al., 2010). Moreover, for the parameters considered here, the growth rate $-k_i^{max}$ is always positive. This means that the plume is always unstable. In this convective instability, the perturbations will grow while they are convected in the direction of the flow. Figure 4b shows that waves are dispersive and the phase velocity $c = \omega / k_r$ weakly depends on V_g. The wavenumber k_r^{max} of the most unstable mode is shown in Figure 5b. Observe that this wavenumber increases with V_g in agreement with our experiments where it was observed that the wavelength of the digitations decrease when the concentration increases.

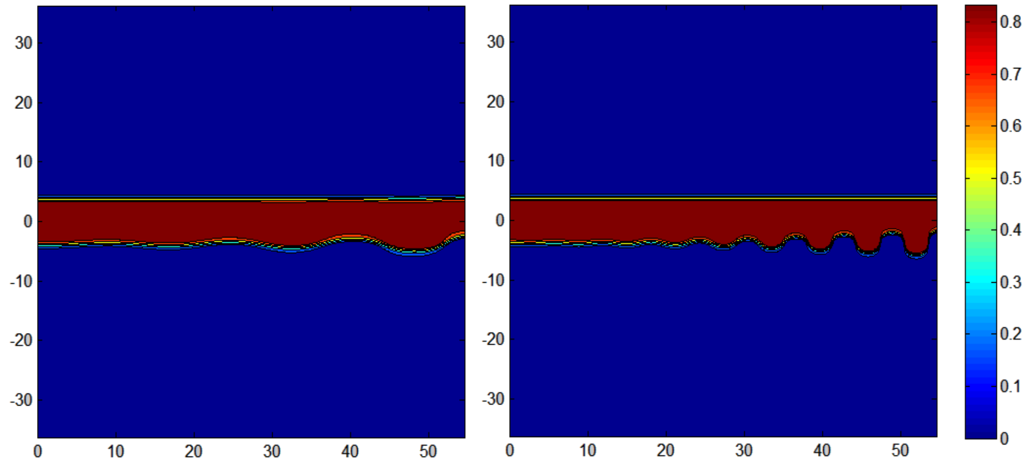

Figure 3. Effect of the anisotropy of the dispersion tensor on the shape of the most unstable mode. The figure shows the normalized concentration field $C_m(x,y)$ of the most unstable mode in the non-isotropic (a) and the isotropic (b) cases (x and y are non-dimensionalized by the gap $b \approx 0.55mm$. The non-dimensional parameters are $Pe = 22$, $\bar{\lambda} = 7.6$ and $Vg = 0.58$

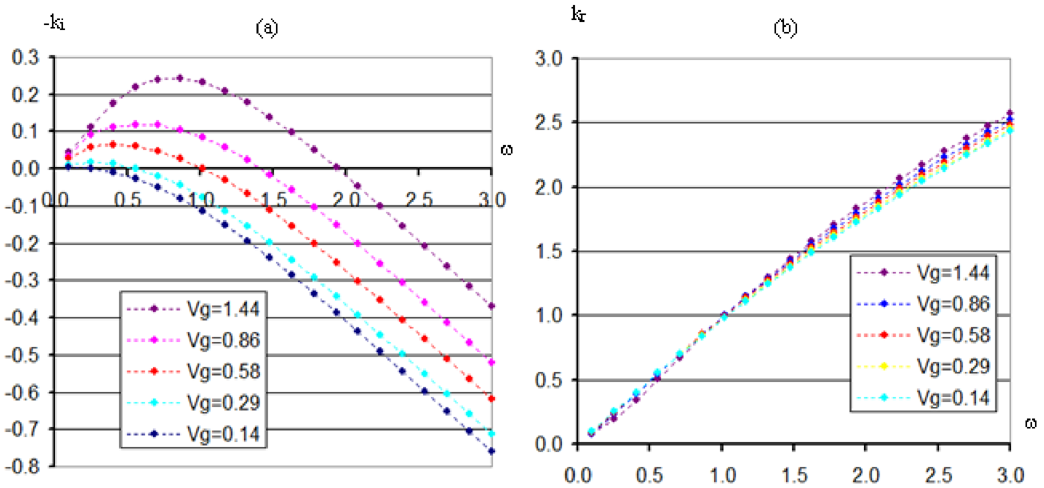

Figure 4. Growth rate $-k_i$ and wavenumber k_r versus the pulsation ω, for various non-dimensional sedimentation velocities V_g. The other non-dimensional parameters are $Pe = 22$, $\bar{\lambda} = 7.6$

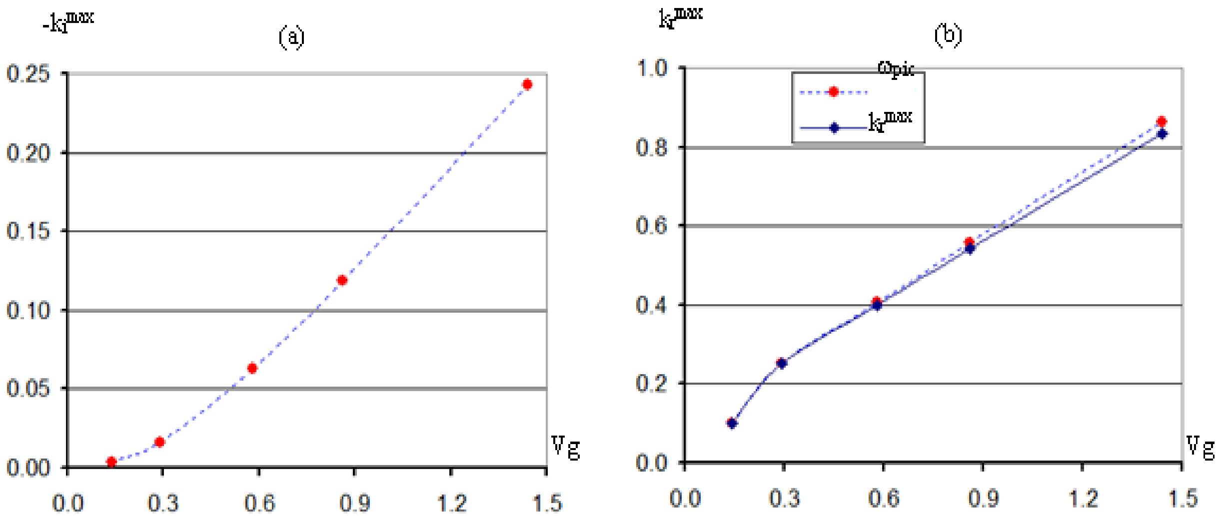

Figure 5. Growth rate $-k_i^{max}$ and wavenumber k_r^{max} of the most unstable mode versus V_g. The other non-dimensional parameters are Pe = 22 and $\bar{\lambda}$ =7.6

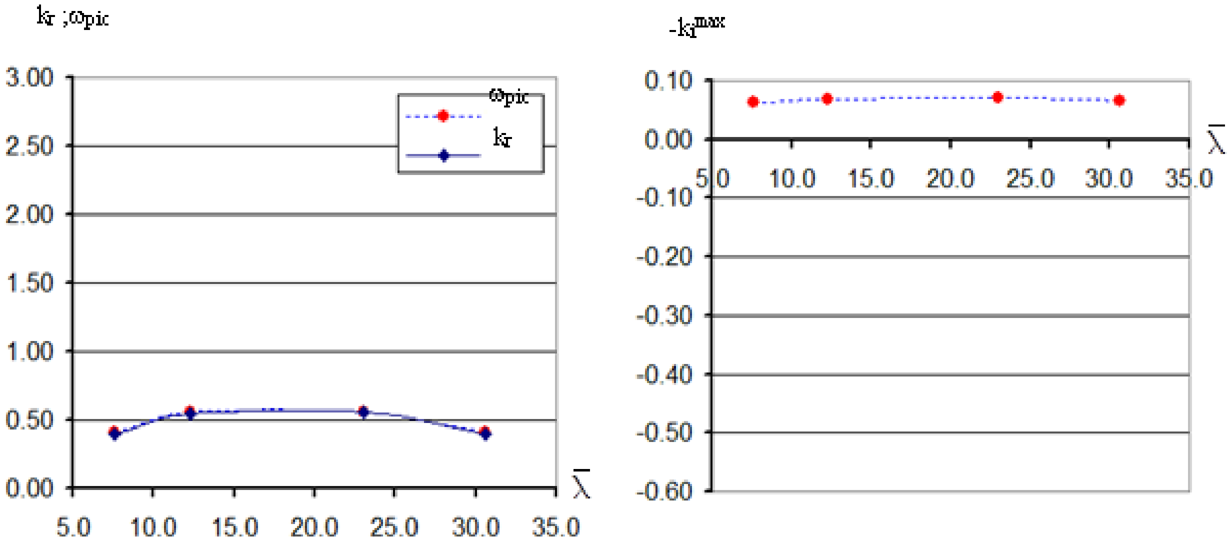

Figure 6. Growth rate (left) and wavenumber (right) of the most unstable mode, when Pe=22, Vg=0.58

5. Influence of the solute flow rate

The effects of the flow rate Q_{inj} on the stability of the plume are considered. Experiments show that the flow rate has little effect on the appearance of the digitations for the parameters examined here. To check whether this trend is visible also in the linear model, The chosen parameters *Pe=22* and *Vg=0.58* are fixed and four values for $\bar{\lambda}$ between 7.6 (Q_{inj} = *0.5 mL/h*) and 30.6 (Q_{inj} = *2 mL/h*) are addressed. Figure 6 shows the growth rate and the wavenumber of the most unstable mode. These quantities remain almost unchanged, whereas the flow rate has been multiplied by 4. As discussed above, this tendency is in qualitative agreement with our experimental results.

6. Influence of the zonal flow

Experiments and simulations (Trieu et al., 2010) suggest that the zonal flow has a "stabilizing effect", as digitations are smaller when one increases the speed V_∞ of the horizontal uniform flow. This observation could be due to the fact that, as V_∞ increases, the plume is transported faster towards the exit of the test zone, so that digitations might not have enough time to develop. In addition, the zonal flow might also have a direct effect on the growth rate $-k_i$. In order to check this, The chosen parameters $\bar{\lambda} = 7.6$, Vg=0.58 are fixed and the parameter Pe is varied between 14.7 and 36.7, which corresponds to the change of velocity $0.06\, mm/s \le V_{\infty} \le 1.2\, mm/s$. Results are shown in Figures 7 and 8. Observe that the zonal flow has a direct and non-negligible effect on the growth rate, the larger the Pe, the smaller the growth rate. This is an indirect effect of the mechanical dispersivity of the medium. This effect is clearly visible in Figure 8 where the growth rate of the most unstable mode is plotted versus Pe. In addition, the wavelength of the most unstable mode increases with Pe.

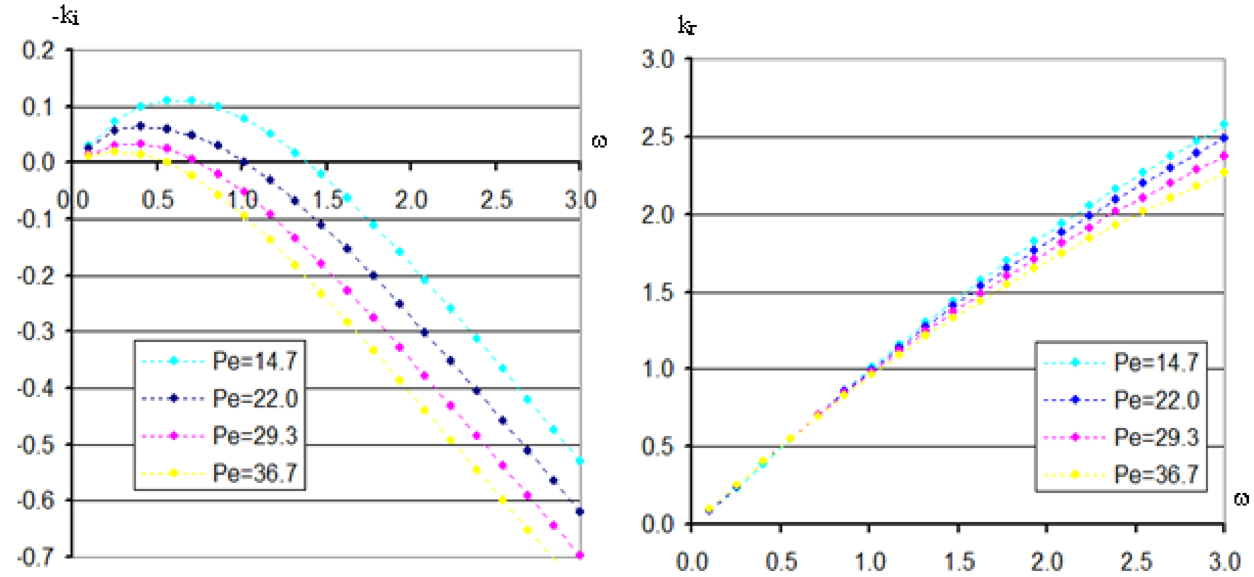

Figure 7. Growth rate (left) and wavenumber (right) when $\bar{\lambda} = 7.6$ and Vg=0.58

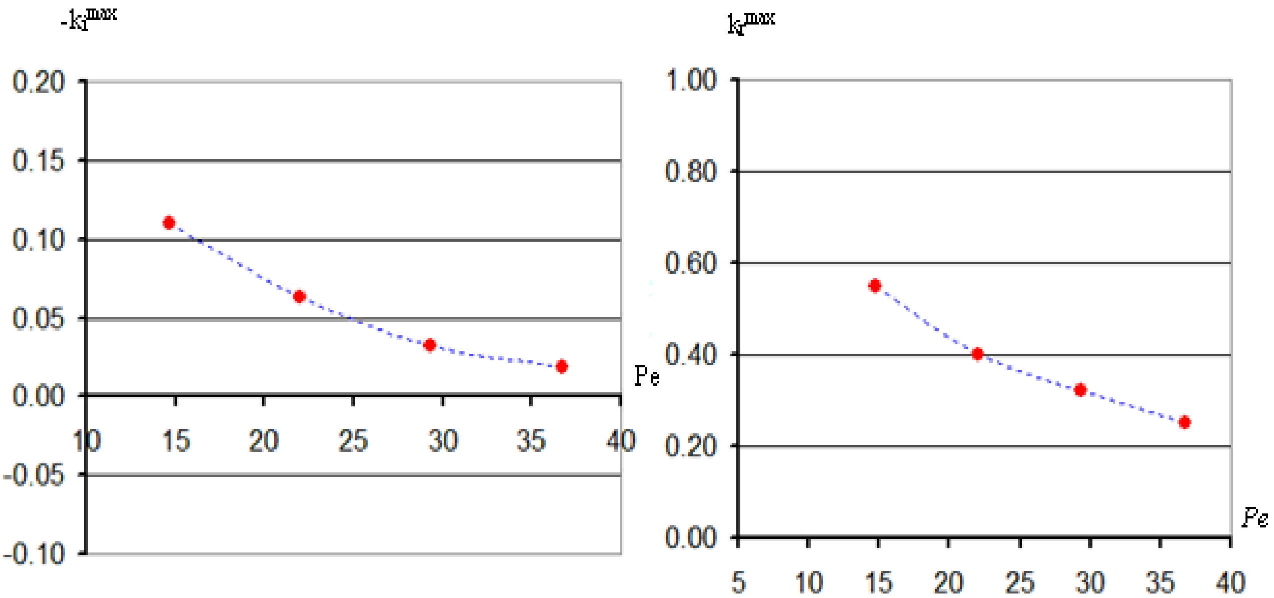

Figure 8. Growth rate (left) and wavenumber (right) of the most unstable mode, when $\bar{\lambda} = 7.6$ and Vg=0.58

7. Conclusion

The stability analysis presented here concerns a parallel quasi-steady flow which can be considered as a rough approximation of the plume investigated in the experiments (Trieu et al., 2010). Nevertheless, if the zonal flow is strong enough, or if the concentration is small enough, the plume has a quasi-horizontal shape (far from the needle through which solute is injected), and the approximation is suitable. In addition, this model flow is controlled by the same parameters as the experimental flow, namely the velocity of the zonal flow, the flow rate and the concentration of the solute injected through the needle. In non-dimensional form, these parameters correspond to the Péclet number Pe, the non-dimensional thickness of the unperturbed plume $\bar{\lambda}$, and the non-dimensional sedimentation velocity V_g. This linear analysis confirms that the various plume configurations strongly depend on Pe and V_g, i.e. on the zonal speed V_∞ and on the injected concentration C_{inj}, in agreement with experiments and numerical simulations. For the parameters considered here, the plume is always convectively unstable as the growth rate of the most unstable mode is always strictly positive as soon as $C_{inj} > 0$. This linear analysis also shows that the Taylor dispersion significantly influences the appearance of digitations. In particular, the longitudinal dispersivity has a stabilizing effect. In addition, we observe that the phase velocity is constant when the dispersion tensor is isotropic, whereas waves are dispersive (the group velocity differs from the phase velocity) when this tensor is non-isotropic. The appearance of an absolute instability in the non-isotropic case, which is linked to the appearance of zeros in the group velocity, is therefore a topic of interest which is among the perspectives of the present work.

REFERENCES

Betchov R., and Criminale W.O., 1967. Stability of parallel flows. Academic Press, New York, London.

Dane, J.H., Güven, O., Oostrom M., HayWorth S. and L eijnse A., 1994. Dense aqueous phase contaminant plume behaviour in porous media near the groundwater table. Future Groundwater Resources at Risk (Proceedings of the Helsinki Conference, June 1994). IAHS Publ. no. 222.

Min Chan Kim., 2015. Theoretical analysis on the onset of buoyancy-driven instability of horizontal interfaces between miscible fluids in a Hele–Shaw cell. Applied Mathematics and Computation, Volume 265, 15 August 2015, pages 207-224.

Oltéan C., Felder Ch., Panfilov M. and Buès M.A., 2004. Transport with a very low density contrast in Hele-Shaw cell and porous media: evolution of the mixing zone. Transp. Porous Media, 55, 339-360.

Schincariol R.A. and Schwartz F.W., 1990. An experimental investigation of variable density flow and mixing in homogeneous and heterogeneous media. Water Resources Research, vol. 26, n° 10, 2317-2329.

Schincariol R.A. and Schwartz F.W., 1994. “On the generation of instabilities in variable density flow”, Water Resources Research, Vol. 30, n° 4, 913-927.

Suslov S.A., 2006. Numerical aspects of searching convective/absolute instability transition. Journal of Computational Physics, 212 :188–217.

Trieu H. T., Oltéan C., Golfier F., and Buès M. A, 2010. Laboratory and numerical investigations of variable density-flow and transport in Hele-Shaw cell. Proceedings of CMWR2010:XVIII International Conference on Computational Methods in Water Resources, Barcelona, Spain, June 21-24.